Department of Analytical Biochemistry, School of Pharmacy, Iwate Medical University, Iwate, Japan

Selective growth suppressive effect of pravastatin on senescent human lung fibroblasts

H. Ushijima*, A. Onodera

Received February 2. 2022, accepted March 3, 2022

**Corresponding author: Hironori Ushijima, Department of Analytical Biochemistry, School of Pharmacy, Iwate Medical University, 1-1-1, Idaidori, Yahaba, Shiwa-gun, Iwate 0283694, Japan. hushijim@iwate-med.ac.jp*

Pharmazie 77: 132-136 (2022) *doi: 10.1691/ph.2022.2327*

Various chemical reagents containing inhibitors of mitochondrial activity, antioxidants, nuclear factor-kappa B (NF-kB) inhibitor, mammalian target of rapamycin (mTOR) inhibitor and other clinical therapeutics were screened in order to identify those that selectively decrease the viability of senescent human lung fibroblasts. Cell viability was measured using the CCK-8 assay. The results showed that pravastatin, a drug for hyperlipidemia, decreased the viability of senescent cells but not non-senescent cells. The effect of pravastatin on senescent cells is thought to be due to the inhibition of cell proliferation, rather than cell death. The effect of pravastatin was further investigated using the glucose metabolism assay, which showed that glucose consumption was inhibited both in non-senescent and senescent cells and intracellular nicotinamide adenine dinucleotide (NAD) was decreased in senescent cells. Changes to the mRNA expression levels of senescence-associated genes in response to pravastatin treatment were quantified by real-time-qPCR. There were no significant changes in the relative mRNA expression levels of IL-1β, p16, p21, and p53 in pravastatin-treated non-senescent cells, whereas the expression of IL-1β and p16 were increased by pravastatin only in senescent cells. The results of this study suggest that pravastatin does not induce senolysis, but rather selectively inhibits the proliferation of senescent cells and that cellular senescence is enhanced by decreasing intracellular NAD and promoting IL-1β production.

1. Introduction

Cellular senescence is caused by exposure to various stressors, including oxidative stress, chemotherapeutic agents, mitochondrial dysfunction, and irradiation (Kuilman et al. 2010). Senescent cells are characterized by arrest of proliferation and increased activities of senescence-associated β-galactosidase and the induction of the senescence-associated secretory phenotype (SASP) (Herranz et al. 2018), which promotes the secretion of various inflammatory cytokines, such as interleukin (IL)-6, IL-8, and C-C motif chemokine ligand 2, by senescent cells, potentially resulting in the growth of cancer cells and chronic inflammation of surrounding tissues. The accumulation of senescent cells has been associated with age-related diseases, such as atherosclerosis, diabetes, fibrosis, and glaucoma (He et al. 2017; Birch et al. 2020).

Two main strategies are commonly employed for the development of anti-aging drugs: (I) inhibition of the SASP and (II) elimination of senescent cells. The former aims to prevent the inflammatory response caused by the SASP of tissues surrounding senescent cells. The thienotriazolodiazepine JQ1, a potent inhibitor of the BET family of bromodomain proteins, is reported to attenuate the SASP by inhibiting bromodomain-containing protein 4 (Tasdemir et al. 2016). The latter aims to selectively induce death of senescent cells via a process known as senolysis.

Senolytic drugs, a new class of drugs that selectively kill senescent cells, have been applied for the treatment of age-related diseases caused by senescent cells. Senescent cells are resistant to apoptosis, and ABT-737, which inhibits expression of the anti-apoptotic factors Bcl-2 and Bcl-xL, selectively kills both senescent human lung fibroblasts (IMR90) and mouse embryonic fibroblasts with irradiation-induced DNA damage (Yosef et al. 2016). ABT-263 (navitoclax), an orally available derivative of ABT-737, is also reported to selectively kill senescent human lung cells (WI-38 and IMR90), renal epithelial cells, and mouse embryonic fibroblasts. Moreover, oral administration of ABT-263 effectively depleted senescent bone marrow hematopoietic stem cells and muscle stem cells in aged mice (Chang et al. 2016). Dasatinib, a tyrosine kinase inhibitor used for treatment of chronic myeloid leukemia, and quercetin, a flavonoid with antioxidant activities, are reported to kill senescent human preadipocytes and umbilical vein endothelial cells, respectively. In addition, oral gavage with both dasatinib and quercetin was shown to reduce the proportion of senescent cells in aged mice (Zhu et al. 2015). However, it remains unclear whether these drugs produce senolytic effects in human patients. A clinical study reported that Bcl-xL-selective inhibitors cause severe thrombocytopenia (Leverson et al. 2015; Wilson et al. 2010) and combination therapy with dasatinib and quercetin did not improve respiratory function in patients with idiopathic pulmonary fibrosis (Justice et al. 2019). Hence, there exist a need to develop safer anti-aging drugs without harmful adverse effects.

The aim of the present study was to screen candidate drugs to selectively decrease the viability of senescent lung fibroblasts. The results indicated that pravastatin, a therapeutic drug for hyperlipidemia, inhibited the growth of senescent lung fibroblasts *in vitro*.

2. Investigations and results

2.1. Pravastatin decreased the viability of senescent cells

Various drugs were screened to identify those with the ability to decrease the viability of senescent cells (Fig. 1). Chemical reagents affecting the function of mitochondria (Mito-TEMPO, mitochondrial division inhibitor 1, lonidamine, and PK11195), antioxidant drugs (idebenone, ubiquinone, carnosic acid, and glutathione), an NF-kB inhibitor (caffeic acid phenethyl ester), and a mTOR inhibitor (AICAR) decreased the viability of both non-senescent and senescent cells to approximately 80%. In addition, screening of drugs prescribed for diabetes (metformin), embolism (apixaban), hyperlipidemia (atorvastatin and pravastatin), epilepsy (zonisamide and valproic acid), and rheumatoid arthritis (auranofin), as well as herbal medicine-derived ingredients (glycyrrhizin, puerarin, and

paeoniflorin) found that only pravastatin selectively decreased the survival rate of senescent cells. The viability of non-senescent cells and senescent cells was reduced to 56% and 41%, respectively, with A1155463, which induces senolysis (Zhu et al. 2017), and to 82.3% and 46% with pravastatin.

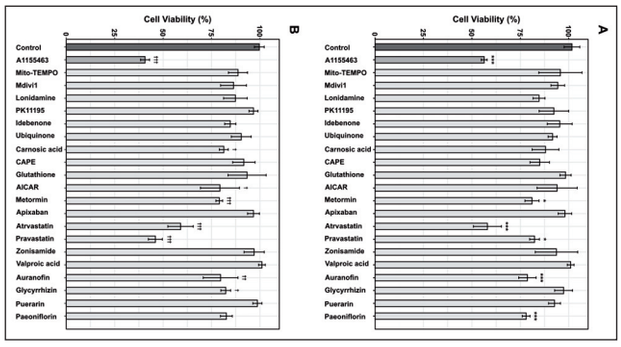

Fig. 1: Screening of chemical compounds that reduce the viability of senescent cells. (A) Non-senescent IMR90 cells and (B) senescent cells were cultured in medium with or without 10 μM tested compounds for 72 h. A1155463 was used as positive control. Cell viability was measured as described in the Materials and Methods section. The values are presented as the mean ± standard deviation (n = 3). Statistical analysis was performed using one-way analysis of variance with Bonferroni correction. *$p < 0.05$ and ***$p < 0.005$ vs. non-senescent control cells, †$p < 0.05$, ††$p < 0.01$, and †††$p < 0.005$ vs. senescent control cells.

2.2. Suppressive effect of pravastatin on the growth of senescent cells

The viability of non-senescent and senescent cells treated with each concentration of pravastatin for 72 h was determined using the CCK-8 assay and compared to that of the control cells (Fig. 2A and B). Pravastatin at concentrations of <2.5 μM maintained the viability of non-senescent cells and senescent cells at 90% or higher. Pravastatin at 10 μM decreased the viability of non-senescent and senescent cells to 72% and 47%, respectively. At pravastatin concentrations of >20 μM, there was little difference in the viability between non-senescent and senescent cells.

The cytotoxicity of pravastatin to non-senescent and senescent cells was assessed using the trypan blue exclusion assay. The results showed that the cytotoxicity of pravastatin to the control cells was approximately 3% and there was no significant difference between the non-senescent and senescent cells at concentrations of ≤20 μM (Fig. 2C and D). The highest cytotoxicity (~7.4%) of pravastatin to both non-senescent and senescent cells was detected at 40 μM.

2.3. Effect of pravastatin on glucose and NAD metabolism of senescent cells

To determine whether pravastatin alters glucose metabolism in non-senescent and senescent cells, glucose concentrations were measured in culture medium with and without 10 μM pravastatin. The results showed that pravastatin increased the glucose concentration of the medium of the non-senescent cells from 1.5 to 1.8 μM and that of senescent cells from 1.9 to 2.6 μM (Fig. 3A). The concentration of lactate, which is produced as a result of glucose metabolism, was also quantified in the culture medium. The results showed that pravastatin increased the amount of lactate in the medium of non-senescent and senescent cells from 2.5 to 3.2 μM and from 3.5 to 4.4, respectively (Fig. 3B). In addition, intracellular NAD, which is an indicator of mitochondrial activity, was also quantified in the medium of non-senescent and senescent cells treated with and without pravastatin. The results showed that pravastatin decreased the amount of intracellular NAD by 24% in senescent cells, but had no effect in non-senescent cells (Fig. 3C). In addition, there was no significant difference in intracellular NADH between the non-senescent and senescent cells (Fig. 3D).

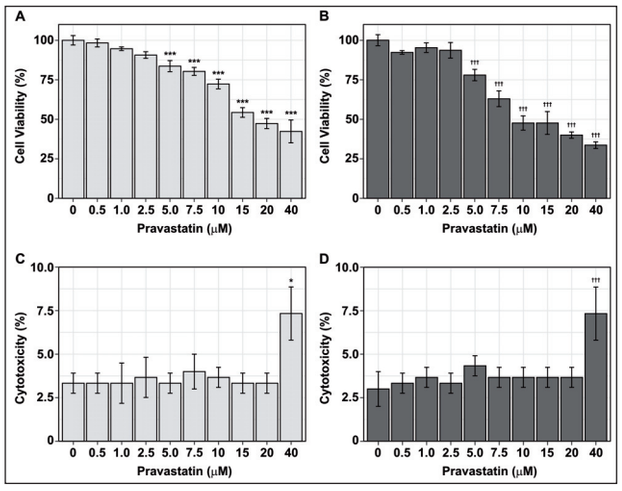

Fig. 2: Pravastatin inhibited the growth of senescent cells. (A and C) Non-senescent cells and (B and D) senescent cells were treated with each concentration of pravastatin for 72 h. Cell viability was determined using the CCK-8 assay. The cytotoxicity of pravastatin to non-senescent and senescent cells was determined with the trypan blue dye exclusion assay after pravastatin treatment for 72 h. The values are presented as the mean ± standard deviation (n = 3). Statistical analysis was performed using one-way analysis of variance with Bonferroni correction. *$p < 0.05$ and ***$p < 0.005$ vs. non-senescent control cells, †††$p < 0.005$ vs. senescent control cells.

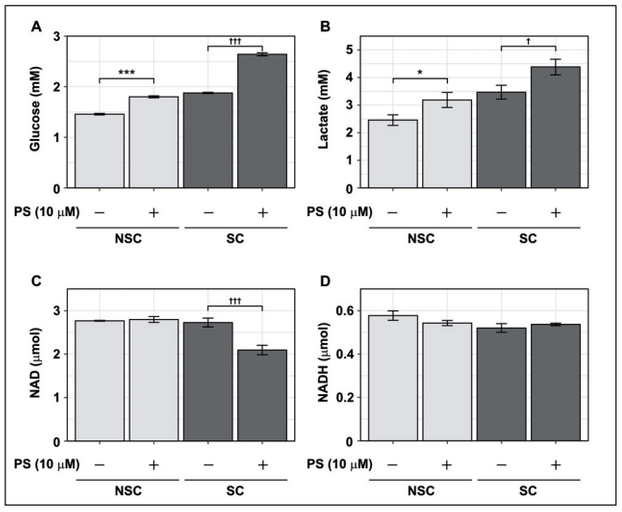

Fig. 3: Pravastatin inhibited glucose and NAD metabolism of senescent cells. (A and B) Non-senescent cells (NSCs) and senescent cells (SCs) were cultured in medium with or without 10 μM pravastatin (PS) for 72 h. The concentrations of glucose and lactate in the medium were determined as described in the Material and Methods section. (C and D) The control and pravastatin-treated cells were collected by trypsin treatment and cell lysates were prepared using NAD/NDAH extraction buffer. The concentrations of total NAD/NADH and NADH in the lysates were determined as described in the Material and Methods section. The values are presented as the mean ± standard deviation (n = 3). Statistical analysis was performed using Student's *t*-test. ***$p < 0.005$ vs. control NSCs, †$p < 0.05$ and †††$p < 0.005$ vs. control SCs.

2.4. Changes in mRNA expression levels of senescence-associated genes by pravastatin treatment

The results presented in Fig. 3 suggest that pravastatin might inhibit mitochondrial activity of senescent cells and a decrease in the amount of NAD might promote cellular senescence. RT-qPCR was performed to investigate changes in the expression levels of the senescence-associated genes IL-1β, IL-6, p16, p21, and p53 in the control and pravastatin-treated cells (Fig. 4). There were no significant changes in the relative mRNA expression levels of IL-1β, p16, p21, and p53 in pravastatin-treated non-senescent cells, whereas pravastatin had increased the relative mRNA expression levels of IL-1β and p16 in senescent cells from 11.7 to 15.4 and

from 1.8 to 2.2, respectively, but decreased the relative mRNA expression of IL-6 from 1.0 to 0.42 in non-senescent cells with no significant change in senescent cells.

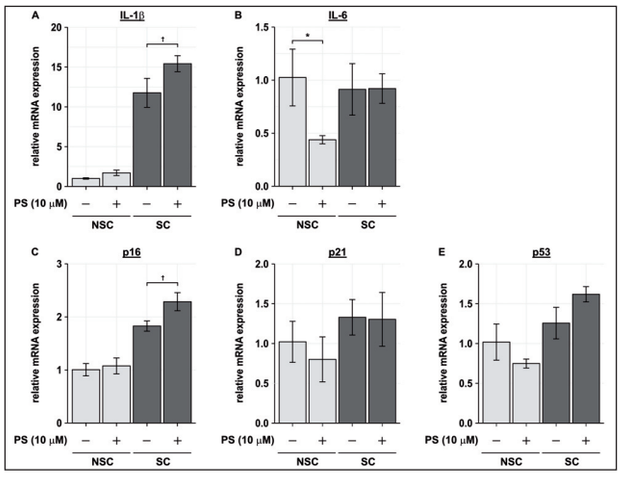

Fig. 4: Pravastatin-induced changes in the expression levels of senescence-associated genes. Non-senescent cells (NSC) and senescent cells (SC) were cultured in the medium with or without 10 μM pravastatin (PS) for 72 h. Total RNA was extracted and reverse-transcribed into cDNA using a reverse transcription kit. The relative mRNA expression levels of IL-1β, IL-6, p16, p21, and p53 in NSC without PS treatment were quantified by RT-qPCR. Values are presented as the mean ± standard deviation (n = 3). Statistical analysis was performed using one-way analysis of variance with Bonferroni correction. *$p < 0.05$ vs. control NSCs, †$p < 0.05$ vs. control SCs.

Table 1: Primers used for RT-qPCR analysis

Target gene	Forward primer	Reverse primer
β-actin	CATGTACGTTGCTATCCAGGC	CTCCTTAATGTCACGCACGAT
IL-1β	AGCCATGGCAGAAGTACCTG	CCTGGAAGGAGCACTTCATCT
IL-6	CCTTCTCCACAATACCC	GTCGAGGATGTACCGA
p16	GAAGGTCCCTCAGACATCCC	GGACCTTCGGTGACTGATGA
p21	TCTTGTACCCTTGTGCCTCG	ATCTGTCATGCTGGTCTGCC
p53	TTCCGAGAGCTGAATGAGGC	TTTGGACTTCAGGTGGCTGG

3. Discussion

In this study, the growth inhibitory effect of pravastatin was assessed in senescent lung fibroblasts and the underlying molecular mechanism was investigated in terms of decreased glucose metabolism, amount of intracellular NAD, and changes to the mRNA expression levels of senescence-associated genes.

The drug screening results showed that only pravastatin inhibited the growth of senescent cells. On the other hand, atorvastatin, which is also used for the treatment of hyperlipidemia, decreased the viability of both non-senescent and senescent cells. It has been reported that atorvastatin possesses more cytotoxic effect than pravastatin to induce cell death via the production of reactive oxygen species (Chen et al. 2016). It suggests that the capacity to reduce cholesterol biosynthesis, which is a common pharmacological action of statins, is less involved in the ability of pravastatin to selectively decrease the viability of senescent cells.

At concentrations of 5 to 10 μM, pravastatin decreased the viability of senescent cells more than that of non-senescent cells. The results of the trypan blue assay suggested that the viability-decreasing effect of pravastatin was not due to the induction of cell death, but rather inhibition of cell proliferation. As compared to other senolytic drugs, such as ABT263 and 17-DMAG (Chang et al. 2016; Fuhrmann-Stroissnigg et al. 2017), which induce death of senescent cells, pravastatin has a milder inhibitory effect on the growth of senescent cells.

Previous studies have reported that decreased glucose metabolism and down-regulation of mitochondrial activity accompanied by decreased intracellular NAD levels are characteristic of senescent cells (Gitenay et al. 2014; Dodson et al. 2013). The results of the present showed that pravastatin suppressed glucose consumption and promoted lactate production in both non-senescent and senescent cells. Pravastatin reduced intracellular NAD concentrations by 24% only in senescent cells, which may contribute to the selective proliferation inhibitory effect against senescent cells. These findings suggest that pravastatin further increases cellular senescence.

The expression levels of the inflammatory cytokines IL-1β and IL-6 are up-regulated in many types of senescent cells and both are secreted extracellularly via the SASP, which is characteristic of senescent cells (Khosla et al. 2020; Birch et al. 2020; De Cecco et al. 2019). In this study, IL-1β mRNA was 11.7-fold greater in senescent cells than non-senescent cells and pravastatin selectively upregulated IL-1β mRNA expression by 32% in the senescent cells. This effect differs from previously reported anti-aging strategies by reducing IL-1β expression (Huang et al. 2020). However, future studies are needed to elucidate the molecular mechanism underlying the selective action of pravastatin on senescent cells and the predicted adverse inflammatory effects of pravastatin-induced increases in IL-1β expression in other tissues. The results also showed that pravastatin decreased IL-6 mRNA expression in senescent cells, but not senescent cells, suggesting the possible involvement of pathways associated with Klotho (an anti-senescent hormone) or STAT3 that induce decreased expression of IL-6 (Xia et al. 2016; Loppnow et al. 2011). It is also possible that these regulatory mechanisms are disrupted in senescent cells, thereby weakening the anti-inflammatory effects of pravastatin. The three proteins p16, p21, and p53 are important factors involved in cell cycle arrest and the expression levels are increased in various senescent cells (Rayess et al. 2012; Jiang et al. 2017). In this study, pravastatin further increased p16 mRNA expression in senescent cells, suggesting that pravastatin does not activate the p21/p53 pathway, but rather a pathway by which IL-1β increases p16 expression (Wang et al. 2020; Philipot et al. 2014). In addition to the replicative senescence model used in this study, exposure to ionizing radiation, doxorubicin treatment, and oncogene transfection (also called oncogene-induced senescence) can also induced senescence in vitro (Li et al. 2018; Mohammadrezaei et al. 2016; Liu et al. 2018). Thus, future studies are warranted to verify the effects of pravastatin with other senescence models.

In conclusion, this is the first report that pravastatin selectively inhibited the proliferation of senescent lung fibroblasts. Further analysis of intracellular NAD turnover and the physiological function of IL-1β in senescent cells will help to better understand the differences in pravastatin sensitivity between non-senescent and senescent cells and aid in the development of drugs to selectively inhibit the growth of senescent cells.

4. Experimental

4.1. Chemicals and materials

Minimum essential medium (MEM), trypsin, fetal bovine serum, and non-essential amino acids were purchased from Thermo Fisher Scientific (Waltham, MA, USA). Dimethyl sulfoxide and pravastatin were obtained from Nacalai Tesque, Inc. (Kyoto, Japan) and FUJIFILM Wako Pure Chemical Industries, Ltd., Osaka, Japan (Osaka, Japan), respectively. Trypan blue was purchased from Bio-Rad Laboratories (Hercules, CA, USA). A1155463 was purchased from Cayman Chemical Company (Ann Arbor, MI, USA). Mito-TEMPO, mitochondrial division inhibitor 1, lonidamine, idebenone, and metformin were purchased from Focus Biomolecules, LLC (Plymouth Meeting, PA, USA). PK11195 was purchased from Santa Cruz Biotechnology, Inc. (Dallas, TX, USA). Ubiquinone, carnosic acid, caffeic acid phenethyl ester, 5-aminoimidazole-4-carboxamide 1-β-D-ribofuranoside (AICAR), atorvastatin, zonisamide, and puerarin were purchased from Tokyo Chemical Industry Co., Ltd. (Tokyo, Japan). Valproic acid, auranofin, and paeoniflorin were purchased from FUJIFILM Wako. Glutathione was purchased from Nacalai Tesque, Inc. Apixaban was purchased from ChemScene, LLC (Monmouth Junction, NJ, USA). Glycyrrhizin was purchased form Kanto Chemical Co., Inc. (Tokyo, Japan). All other chemicals were of the highest commercially available grade.

4.2. Cell culture

Human lung fibroblasts (IMR90 and IMR90-40) were obtained from the Japanese Collection of Research Bioresources Cell Bank (Osaka, Japan) and verified as free of mycoplasma contamination. Cells were cultured in MEM containing 10% (v/v) fetal bovine serum, 1% (v/v) non-essential amino acids, and antibiotics (0.07 g/L penicillin G and 0.1 g/L streptomycin) at 37°C under a humidified atmosphere of 5% CO_2/95%

air. IMR90 cells (population doubling level of 28) were used as non-senescent cells in this study. To induce replicative senescence, IMR90-40 cells were cultured until the population doubling level was >50, their cells were used as senescent cells (Jin et al. 2013). Cell proliferation was monitored using a TC10 automated cell counter (Bio-Rad Laboratories).

4.3. Measurement of cell viability

The Cell Counting Kit-8 (CCK-8) with water-soluble tetrazolium salts (WST-8; Dojindo Laboratories Co., Ltd., Kumamoto, Japan) was used to measure the viability of non-senescent and senescent cells in accordance with the manufacturer's protocol. Stock solutions of the tested compounds were all prepared in dimethyl sulfoxide. Briefly, cells were seeded into the wells of a 96-well microplate (3×10^3 cells/well). After 24 h, the medium was replaced with fresh medium containing different concentrations of the tested compounds, followed by further incubation for 72 h. The control groups of non-senescent and senescent cells were incubated with medium containing 0.1% dimethyl sulfoxide. CCK-8 solution (10 µL) was added to each well and the plates were incubated for 3 h at 37°C under an atmosphere of 5% CO_2/95% air. Absorbance was measured at 490 nm using an iMark microplate reader (Bio-Rad Laboratories).

4.4. Measurement of cytotoxicity of pravastatin

The cytotoxicity of pravastatin to non-senescent or senescent cells was measured using the trypan blue dye exclusion assay (Strober 2001). Cells were treated with different concentrations of pravastatin for 72 h and harvested using 0.25% trypsin. An aliquot of the cell suspension stained with 0.4% trypan blue (Bio-Rad Laboratories) was transferred to a cell counting slide and the ratio of living to dead cells was measured using a TC10 automated cell counter.

4.5. Measurement of glucose and lactate concentrations

Cells (6×10^3 cells/well) were seeded into the wells of a 96-well microplate and precultured for 24 h at 37°C under an atmosphere of 5% CO_2/95% air. Subsequently, the medium was replaced with fresh medium with or without 10 µM pravastatin and the cells were cultured for an additional 72 h. The cell supernatant was transferred to the wells of a 96-well plate and the concentrations of glucose and lactate were determined using the Glucose Assay Kit-WST (Dojindo Laboratories Co., Ltd.) and Lactate Assay Kit-WST (Dojindo Laboratories Co., Ltd.), respectively. Absorbance was measured at 450 nm using an iMark microplate reader (Bio-Rad Laboratories) and the concentrations of glucose and lactate were calculated based on calibration curves.

4.6. Measurement of intracellular nicotinamide adenine dinucleotide (NAD)/NADH concentrations

NAD/NADH concentrations were determined using a NAD/NADH assay kit (Dojindo Laboratories Co., Ltd.). In brief, cells (1.2×10^5 cells) were seeded on a 100-mm dish and precultured for 24 h at 37°C under an atmosphere of 5% CO_2/95% air. Subsequently, the medium was replaced with fresh medium with or without 10 µM pravastatin. After 72 h, the cells were harvested with 0.25% trypsin and cell lysates were prepared using NAD/NADH extraction buffer. The lysates were transferred to filtration tubes (molecular weight cut-off of 10 kDa) and centrifuged at 12,000 × *g* for 10 min. The filtrates were collected and divided into two samples each to determine the NAD/NADH ratio and NADH concentration, respectively. After the sample solutions were reacted with WST-enzyme working solution, the amounts of total NAD/NADH and NADH in the samples were calculated by measuring the absorbance at 450 nm using an iMark microplate reader (Bio-Rad Laboratories).

4.7. Quantification of mRNA expression

Cells were cultured in MEM with or without 10 µM pravastatin. After 72 h, total RNA was extracted from the control and pravastatin-treated cells using the RNeasy mini kit (Qiagen, Hilden, Germany) and 1 mg was reverse-transcribed into cDNA using ReverTra Ace qPCR RT master mix (Toyobo Co., Ltd., Osaka, Japan). mRNA expression was quantified by real-time quantitative polymerase chain reaction (RT-qPCR) with TB Green Premix Ex Taq II polymerase (Takara Bio, Shiga, Japan) and an Eco Real-Time PCR System (Illumina, Inc., San Diego, CA, USA). The relative expression of each mRNA was calculated using the $2^{-\Delta\Delta Ct}$ method (Livak et al. 1997) and normalized to that of β-actin. The sequences of the primer sets used in this assay are listed in Table 1.

4.8. Statistical analyses

Statistical analyses were conducted using the R Project for Statistical Computing (https://www.r-project.org/). One-way analysis of variance with Bonferroni correction was used to identify significant differences in cell viability, cytotoxicity of pravastatin, and differences in relative mRNA expression between the control and pravastatin-treated groups. The Student's *t*-test was used to assess significant changes in glucose metabolism. A probability (p) value of <0.05 was considered statistically significant.

Acknowledgments This research was supported by the Japan Society for the Promotion of Science (KAKENHI grant no. 19K11749) and a scientific research grant from Iwate Medical University.

Conflict of Interest: The authors have no conflicts of interest or any competing financial interest to declare.

Author Contributions: Hironori Ushijima: Conceptualization, Methodology, Investigation, Resources, Data curation, Validation, Formal analysis, Visualization, Supervision, Writing, Funding acquisition, and Project administration. Arisa Onodera: Methodology, Investigation, Data curation, Validation, Formal analysis, and Visualization.

References

Birch J, Gil J (2020) Senescence and the SASP: many therapeutic avenues. Genes Dev 34: 1565–1576.

Chang J, Wang Y, Shao L, Laberge RM, Demaria M, Campisi J, Janakiraman K, Sharpless NE, Ding S, Feng W, Luo Y, Wang X, Aykin-Burns N, Krager K, Ponnappan U, Hauer-Jensen M, Meng A, Zhou D (2016) Clearance of senescent cells by ABT263 rejuvenates aged hematopoietic stem cells in mice. Nat Med 22: 78–83.

Chen YH, Chen YC, Liu CS, Hsieh MC (2016) The different effects of atorvastatin and pravastatin on cell death and PARP activity in pancreatic NIT-1 Cells. J Diabetes Res 2016: 1828071.

De Cecco M, Ito T, Petrashen AP, Elias AE, Skvir NJ, Criscione SW, Caligiana A, Brocculi G, Adney EM, Boeke JD, Le O, Beauséjour C, Ambati J, Ambati K, Simon M, Seluanov A, Gorbunova V, Slagboom PE, Helfand SL, Neretti N, Sedivy JM (2019) L1 drives IFN in senescent cells and promotes age-associated inflammation. Nature 566: 73–78.

Dodson M, Darley-Usmar V, Zhang J (2013) Cellular metabolic and autophagic pathways: traffic control by redox signaling. Free Radic Biol Med 63: 207–221.

Fuhrmann-Stroissnigg H, Ling YY, Zhao J, McGowan SJ, Zhu Y, Brooks RW, Grassi D, Gregg SQ, Stripay JL, Dorronsoro A, Corbo L, Tang P, Bukata C, Ring N, Giacca M, Li X, Tchkonia T, Kirkland JL, Niedernhofer LJ, Robbins PD (2017) Identification of HSP90 inhibitors as a novel class of senolytics. Nat Commun 8: 422.

Gitenay D, Wiel C, Lallet-Daher H, Vindrieux D, Aubert S, Payen L, Simonnet H, Bernard D (2014) Glucose metabolism and hexosamine pathway regulate oncogene-induced senescence. Cell Death Dis 5: e1089.

He S, Sharpless NE (2017) Senescence in Health and Disease. Cell 169: 1000–1011.

Herranz N, Gil J (2018) Mechanisms and functions of cellular senescence. J Clin Invest 128: 1238–1246.

Huang X, You Y, Xi Y, Ni B, Chu X, Zhang R, You H (2020) p-Coumaric acid attenuates IL-1β-induced inflammatory responses and cellular senescence in rat chondrocytes. inflammation 43: 619–628.

Jiang C, Liu G, Luckhardt T, Antony V, Zhou Y, Carter AB, Thannickal VJ, Liu RM (2017) Serpine 1 induces alveolar type II cell senescence through activating p53-p21-Rb pathway in fibrotic lung disease. Aging Cell 16: 1114–1124.

Jin J, Zhang T (2013) Effects of glucose restriction on replicative senescence of human diploid fibroblasts IMR-90. Cell Physiol Biochem 31: 718–727.

Justice JN, Nambiar AM, Tchkonia T, LeBrasseur NK, Pascual R, Hashmi SK, Prata L, Masternak MM, Kritchevsky SB, Musi N, Kirkland JL (2019) Senolytics in idiopathic pulmonary fibrosis: Results from a first-in-human, open-label, pilot study. EBioMedicine 40: 554–563.

Khosla S, Farr JN, Tchkonia T, Kirkland JL (2020) The role of cellular senescence in ageing and endocrine disease. Nat Rev Endocrinol 16: 263–275.

Kuilman T, Michaloglou C, Mooi WJ, Peeper DS (2010) The essence of senescence. Genes Dev 24: 2463–2479.

Leverson JD, Phillips DC, Mitten MJ, Boghaert ER, Diaz D, Tahir SK, Belmont LD, Nimmer P, Xiao Y, Ma XM, Lowes KN, Kovar P, Chen J, Jin S, Smith M, Xue J, Zhang H, Oleksijew A, Magoc TJ, Elmore SW, Souers AJ (2015) Exploiting selective BCL-2 family inhibitors to dissect cell survival dependencies and define improved strategies for cancer therapy. Sci Transl Med 7: 279ra40.

Li M, You L, Xue J, Lu Y (2018) Ionizing radiation-induced cellular senescence in normal, non-transformed cells and the involved DNA damage response: a mini review. Front Pharmacol 9: 522.

Liu XL, Ding J, Meng LH (2018) Oncogene-induced senescence: a double edged sword in cancer. Acta Pharmacol Sin 39: 1553–1558.

Livak KJ, Schmittgen TD (1997) Analysis of relative gene expression data using real-time quantitative PCR and the 2(-Delta Delta C(T)) Method. Methods 21: A.3B.1 – A.3B.2.

Loppnow H, Zhang L, Buerke M, Lautenschläger M, Chen L, Frister A, Schlitt A, Luther T, Song N, Hofmann B, Rose-John S, Silber RE, Müller-Werdan U, Werdan K (2011) Statins potently reduce the cytokine-mediated IL-6 release in SMC/MNC cocultures. J Cell Mol Med 15: 994–1004.

Mohammadrezaei FM, Movaghar AF, Gharghabi M (2016) The effect of caffeine and chk2 inhibitor on doxorubicin-induced cellular senescence in MCF-7 cells. Drug Res 66: 450–454.

Philipot D, Guérit D, Platano D, Chuchana P, Olivotto E, Espinoza F, Dorandeu A, Pers YM, Piette J, Borzi RM, Jorgensen C, Noel D, Brondello JM (2014) p16INK4a and its regulator miR-24 link senescence and chondrocyte terminal differentiation-associated matrix remodeling in osteoarthritis. Arthritis Res Ther 16: R58.

Rayess H, Wang MB, Srivatsan ES (2012) Cellular senescence and tumor suppressor gene p16. Int J Cancer 130: 1715–1725.

Strober W (2001) Trypan blue exclusion test of cell viability. Curr Protoc Immunol Appendix 3: Appendix 3B.

Tasdemir N, Banito A, Roe JS, Alonso-Curbelo D, Camiolo M, Tschaharganeh DF, Huang CH, Aksoy O, Bolden JE, Chen CC, Fennell M, Thapar V, Chicas A, Vakoc CR, Lowe SW (2016) BRD4 Connects Enhancer Remodeling to Senescence Immune Surveillance. Cancer Discov 6: 612–629.

Wang X, Zhang S, Dong M, Li Y, Zhou Q, Yang L (2020) The proinflammatory cytokines IL-1β and TNF-α modulate corneal epithelial wound healing through p16Ink4a suppressing STAT3 activity. J Cell Physiol 235: 10081–10093.

Wilson WH, O'Connor OA, Czuczman MS, LaCasce AS, Gerecitano JF, Leonard JP, Tulpule A, Dunleavy K, Xiong H, Chiu YL, Cui Y, Busman T, Elmore SW, Rosenberg SH, Krivoshik AP, Enschede SH, Humerickhouse RA (2010) Navitoclax, a targeted high-affinity inhibitor of BCL-2, in lymphoid malignancies: a phase 1 dose-escalation study of safety, pharmacokinetics, pharmacodynamics, and antitumour activity. Lancet Oncol 11: 1149–1159.

Xia W, Zhang A, Jia Z, Gu J, Chen H (2016) Klotho contributes to pravastatin effect on suppressing IL-6 production in endothelial cells. Mediators Inflamm 2016: 2193210.

Yosef R, Pilpel N, Tokarsky-Amiel R, Biran A, Ovadya Y, Cohen S, Vadai E, Dassa L, Shahar E, Condiotti R, Ben-Porath I, Krizhanovsky V (2016) Directed elimination of senescent cells by inhibition of BCL-W and BCL-XL. Nat Commun 7: 11190.

Zhu Y, Tchkonia T, Pirtskhalava T, Gower AC, Ding H, Giorgadze N, Palmer AK, Ikeno Y, Hubbard GB, Lenburg M, O'Hara SP, LaRusso NF, Miller JD, Roos CM, Verzosa GC, LeBrasseur NK, Wren JD, Farr JN, Khosla S, Stout MB, McGowan SJ, Fuhrmann-Stroissnigg H, Gurkar AU, Zhao J, Colangelo D, Dorronsoro A, Ling YY, Barghouthy AS, Navarro DC, Sano T, Robbins PD, Niedernhofer LJ, Kirkland JL (2015) The Achilles' heel of senescent cells: from transcriptome to senolytic drugs. Aging Cell 14: 644–658.

Zhu Y, Doornebal EJ, Pirtskhalava T, Giorgadze N, Wentworth M, Fuhrmann-Stroissnigg H, Niedernhofer LJ, Robbins PD, Tchkonia T, Kirkland JL (2017) New agents that target senescent cells: the flavone, fisetin, and the BCL-XL inhibitors, A1331852 and A1155463. Aging 9: 955–963.